




Artificial Neural Network Approach to Determine Elastic Modulus of Carbon Fiber-Reinforced Laminates

XIANBO XU ^{1,2} and NIKHIL GUPTA¹

1.—Composite Materials and Mechanics Laboratory, Mechanical and Aerospace Engineering Department, New York University Tandon School of Engineering, 6 Metrotech Center, Brooklyn, NY 11201, USA. 2.—e-mail: xianbo.xu@nyu.edu

Recognized as a prominent material for engineering applications, carbon fiber-reinforced laminated composites require significant effort to characterize due to their anisotropic structure and viscoelastic nature. Dynamic mechanical analysis has been used to accelerate the testing process by transforming the measured viscoelastic properties to elastic modulus. To expand the transformation to anisotropic materials, artificial neural network approach is used to build the master relationship of the storage modulus in three in-plane directions. Using rotation transformation, the stiffness tensor can be calculated to extrapolate the frequency domain viscoelastic properties in any orientation with respect to the fiber direction. The viscoelastic properties are transformed to time domain relaxation function using the linear relationship of viscoelasticity. Stress response with a certain strain history is predicted and the elastic modulus is extracted. Compared to the experimental flexural test results, the artificial neural network-based method achieved an error of less than 7.3%. The results show that the transformation can predict the anisotropic material behavior at a wide range of temperatures and strain rates.

INTRODUCTION

The ability to tailor the properties of composite materials is their biggest asset. However, the directional properties of fiber-reinforced composites require investing significant effort in their characterization.¹ Carbon fiber-reinforced polymer (CFRP) composites with laminated structures are now used in a wide range of structural applications, including aircraft, automobiles,² and sports equipment. Due to their anisotropic properties, laminated composites need to be characterized in several different orientations. The complexity in their characterization increases if the properties are also required over a range of temperatures and strain rates.^{3,4} The elastic modulus is the most important design parameter, which is often the focus of the characterization efforts.⁵ However, conducting a large number of tensile or bending tests with respect to fiber direction, temperature, and strain rate to determine the modulus can be a prohibitively expensive or time consuming.⁶ The strong

viscoelasticity of polymers even within the quasi-static strain rate range also presents a challenge and requires developing a rigorous testing regime.⁷

Viscoelasticity is widely displayed by a large variety of materials, including polymers,⁸ composites⁹ and biomaterials.¹⁰ Viscoelastic properties are commonly characterized by tensile or flexural tests and dynamic mechanical analysis (DMA).^{7,11,12} Tensile and flexural tests can provide Young's modulus, which can be used in mechanical design. However, a large number of specimens need to be tested if the mechanical properties need to be characterized with respect to strain rates.^{3,13,14} The campaign will grow exponentially when testing anisotropic materials. In contrast, the storage (E') and loss (E'') moduli obtained from DMA describe the in-phase and out-of-phase relationships between stress and strain when a sinusoidal load is applied.¹⁵ However, applications of E' and E'' are limited because they are obtained in the frequency domain and do not provide a direct correlation with Young's modulus.

Theoretical models are now available to transform the storage modulus into the elastic modulus.^{16–18} These models require the DMA results to satisfy the time–temperature superposition principle to develop a master curve. The shape of the master curve is modeled by a mathematical function with respect to frequency, which is then transformed to the time domain. This procedure allows the obtaining of the elastic modulus over a large range of strain rates and eliminates the need to conduct a large number of tensile tests at various strain rates.¹⁹ This transformation procedure has been verified on isotropic materials, such as neat polymers,^{16,18,20} syntactic foams¹⁷ and nanocomposites.²¹ However, these methods have not been extended to anisotropic material systems, which require setting up a generalized Hooke’s law-based material model. The artificial neural network (ANN) approach has been used recently in this field to model the material behavior, and has promise to be applied to materials with complex behaviors.^{22–24} The ANN approach has a strong physical foundation²⁵ and is good at handling complex thermal behaviors.^{26,27} It is also the paradigm of parallel computing and robustly enables massive computation tasks,^{28,29} which is a major advantage in modeling complex material responses.^{30,31}

In the current work, a unidirectional CFRP laminate is used as the anisotropic material system to implement the ANN approach and use DMA data to extract the elastic modulus with respect to strain rate in different orientations with respect to the fiber direction. A feed-forward neural network is applied to build the master relationship of E' in different in-plane orientations. The viscoelastic properties can be used to calculate the frequency domain stiffness tensor in the testing direction using rotation transformation.³² Then, using rotation transformation again, the viscoelastic properties in any orientation can be predicted. The frequency domain viscoelastic properties are transformed to a time domain relaxation function using the linear relationship of viscoelasticity and then the time domain elastic modulus is predicted. Since the materials are tested with the aim of finding a correlation between the test methods, the quality of the material is not a study parameter and the transformation should yield accurate results for any material regardless of composition and quality.

MATERIALS AND METHODS

ANN Methodology

The ANN framework is used to establish the master relationship of the storage modulus with respect to frequency and temperature. A feed-forward neural network is used in this work and the general loss function is defined as:³³

$$\tilde{F}(E'; \omega, T) = F(E'; \omega, T) + \alpha\Omega(\mu) \quad (1)$$

where E' is the storage modulus at a certain temperature T and frequency ω , μ represents the network weights, Ω is the regularization term, and α is the corresponding regularization factor. The ratio of the predicted storage modulus (\tilde{E}') to the experimental E' measurement is used to define the prediction error, and the L^2 regularization, or so-called ridge regression, is used as the regularization term as in:³⁴

$$F(E'; \omega, T) = \frac{1}{N} \sum_{i=1}^N \left[\left(\tilde{E}'(\omega, T) / E'(\omega, T) - 1 \right) \right]^2 \quad (2.a)$$

$$\Omega(\mu) = \frac{1}{n} \sum_{j=1}^n \mu_j^2 \quad (2.b)$$

where N is the size of the dataset and n is the number of parameters. Temperature and the logarithmic form of frequency are used as the input neurons. As three is the minimal number to implement the transformation and predict the performance in other orientations for CFRP, the ANN has three output neurons to describe the properties in three orientations ($\theta = 0^\circ, 45^\circ$ and 90°). The definition of the orientations are shown in Fig. 1a and the flow chart of the process is shown in Fig. 1b. Following previous work,²² the ANN has only one hidden layer with two neurons and the regulation factor is set to be 10^{-4} . The number of neurons and regulation factors are not considered as variables for optimization in this work.

The datasets obtained from the DMA tests of the laminates in three orientations ($\theta = 0^\circ, 45^\circ$ and 90°) are each randomly divided into training, validation and test sets in the ratio of 65:15:20, respectively. As a metaheuristic optimization method, particle swarm optimization (PSO)³⁵ has proved to be efficient and robust in solving many nonlinear optimization problems.^{36–38} Hence, PSO is used to train the ANN in this work. Then, using the linear viscoelastic theory, the $E'(\omega, T)$ in each orientation is transformed to the time domain relaxation function $E(t, T)$. The stress response is found by integrating $E(t, T)$ with the strain history, and the elastic modulus in the time domain is extracted.

The Materials and Experiment Procedure

The unidirectional CFRP laminates of 1.6 mm thickness were procured from Allred and Associates, Elbridge, New York, NY, USA. Laminate parameters such as the number of layers and fiber content and defects are not characterized because they are not of relevance to the present work, which is focused on comparing the mechanical property results obtained from two different characterization methods.

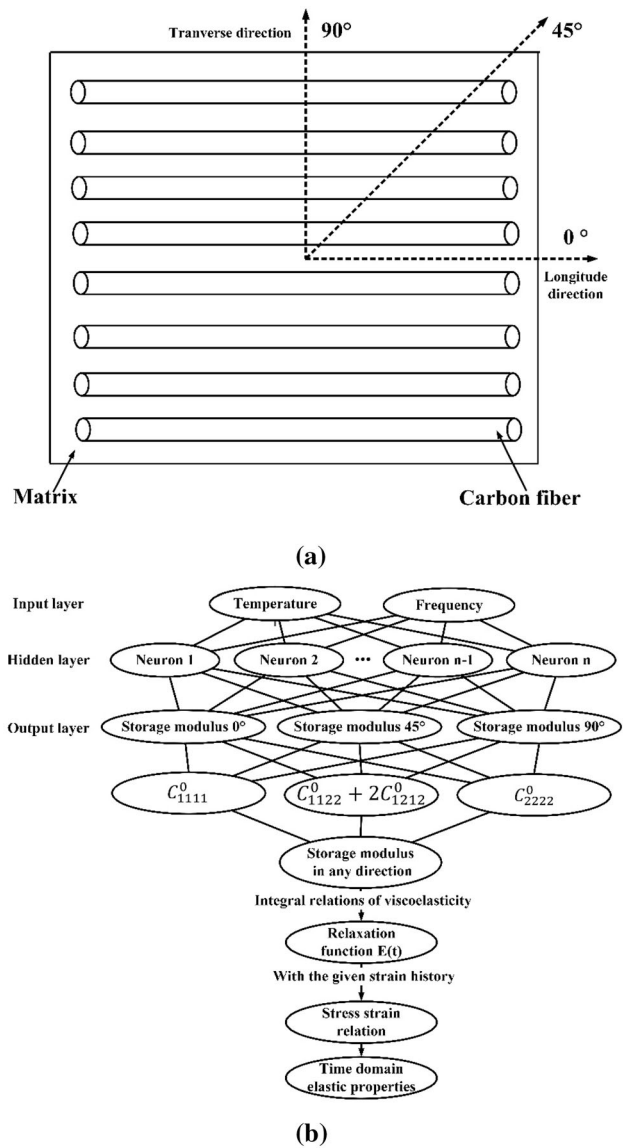


Fig. 1. (a) Definition of 0°, 45° and 90° orientations with respect to the fiber direction in the laminate and (b) the modeling framework using artificial neural network approach.

The laminates were machined into specimens of dimensions $60.0 \times 12.7 \times 1.6 \text{ mm}^3$ (length \times width \times height) in 0°, 45° and 90° orientations for DMA testing. TA Instruments (New Castle, DE, USA) Q800 DMA has been used to conduct the experiments under strain control mode in dual cantilever configuration with a maximum displacement of $25 \mu\text{m}$ using a span length of 35 mm. The tests were conducted in the temperature range of 30–200°C with a step of 5°C and a soaking time of 5 min. Isothermal frequency sweeps were conducted at 20 discrete frequencies logarithmically spaced between 1 and 100 Hz. The experiment was terminated when the force magnitude dropped below 10^{-4} N . The response surface of the storage

modulus with respect to temperature and frequency is presented in Fig. 2. It can be observed that E' decreases with temperature and increases with frequency. The E' at 100 Hz is higher than that at 1 Hz for each temperature in each orientation, which indicates the strain rate sensitivity of the materials. It is also observed in this figure that the storage modulus in 0° is at least 2 times higher than that in 45° and 9 times higher than that in 90°. The obvious directionality is due the anisotropic nature of the material.

The experimental flexural properties are obtained by flexural tests under three-point bending conditions in $\theta = 0^\circ, 45^\circ$ and 90° orientations at room temperature (25°C). An Instron 4467 universal test system was used for the tests at different deflection rates from 1×10^{-3} – $1 \text{ mm} \cdot \text{s}^{-1}$ (nominal initial strain rates of 3×10^{-6} – $3 \times 10^{-3} \text{ s}^{-1}$). The geometry of the specimens conforms to the ASTM D790 standard.³⁹ A representative set of stress–strain curves for a unidirectional CFRP laminate in 0°, 45° and 90° orientation (deformation rate of 1 mm/s) is shown in Fig. 3. Further, flexural tests on the laminate were also conducted in $\theta = 30^\circ$ orientation. The data obtained in this orientation have been used for validation of the results obtained from the ANN-based model which was developed using the data in the 0°, 45° and 90° orientations. At least three specimens were repeated for each strain rate and orientation, and data for all three specimens are included in the plots.

Transformation of Storage Modulus to Time Domain

For anisotropic elastic materials, the stress and strain are related to the stiffness tensor in both the time and frequency domains and the relationship can be written using Einstein summation notation as:

$$\sigma_{ij} = C_{ijkl} \varepsilon_{kl} \quad (3)$$

where σ is the stress tensor, ε is the strain tensor, and C is the stiffness tensor. The stiffness tensor is dependent on θ . The CFRP laminate is commonly regarded as a thin-shell structure and its stiffness properties can be found by calculating only the in-plane component of the stiffness tensor. The elasticity term for axial properties under a rotation transformation can be found using:⁴⁰

$$C_{1111}^0 = C_{1111}^0 \cos^4 \theta + 2(C_{1122}^0 + 2C_{1212}^0) \cos^2 \theta \sin^2 \theta + C_{2222}^0 \sin^4 \theta \quad (4)$$

C_{1111} , C_{1122} , C_{1212} , and C_{2222} correspond to C_{11} , C_{12} , C_{66} , and C_{22} , respectively, when using a 2-index notation. Although the stiffness properties in certain orientations are related to four components of the stiffness tensor, they are linearly dependent on three terms in Eq. 4. Rather than calculating all the

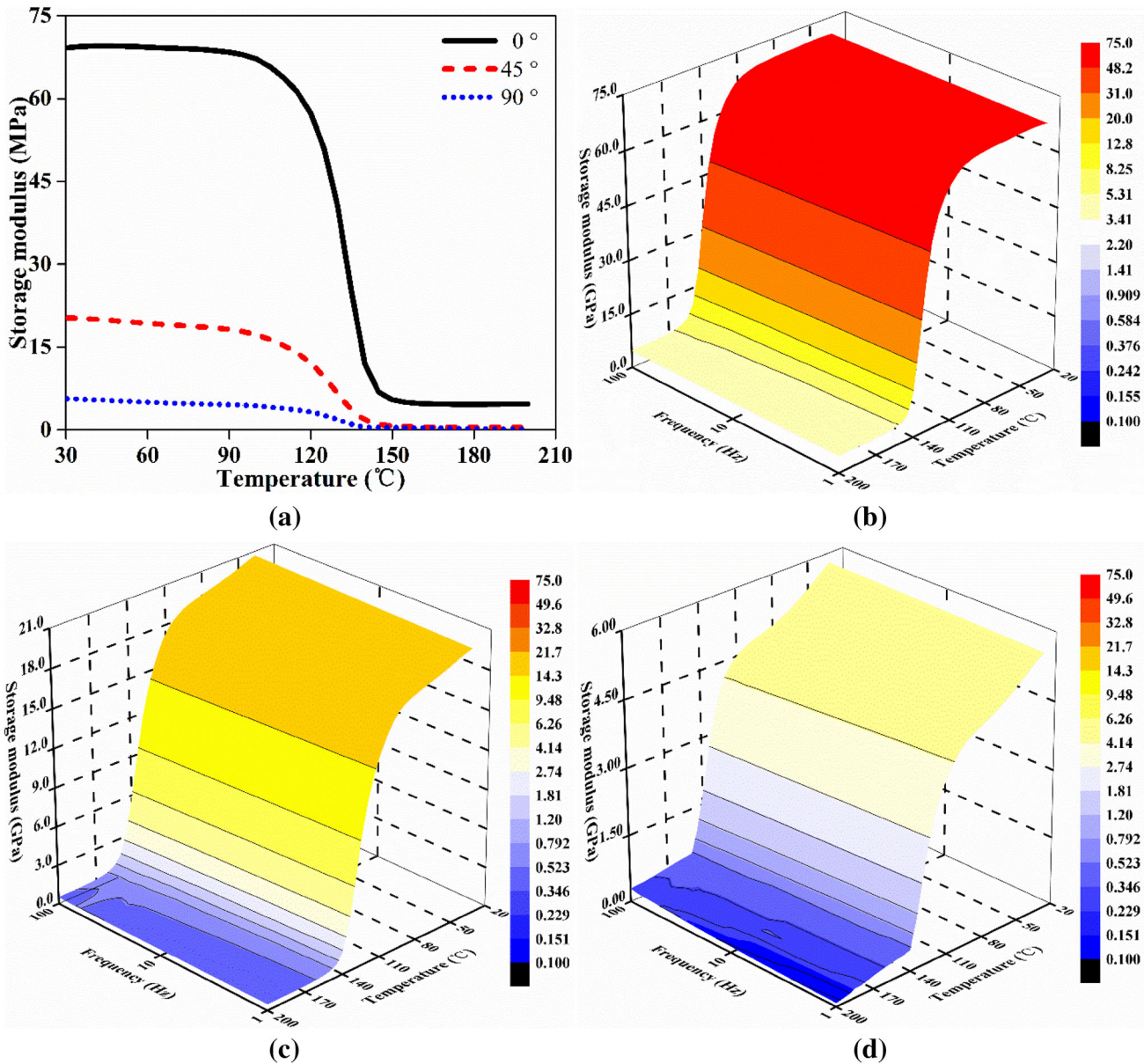


Fig. 2. (a) The trend of storage modulus with respect to temperature at 1 Hz frequency for three orientations of laminates shown in Fig. 1a. Response surface of storage modulus measured with respect to temperature and frequency in (b) 0°, (c) 45° and (d) 90° orientation.

four components of the stiffness tensor, the three terms can be calculated using the test data of three orientations and used to predict the axial stiffness in any orientation. The DMA results in three orientations are used to train the ANN with the PSO algorithm, and the training errors of the tests set in all three orientations are found to be below 5.4%. The Pearson's correlation coefficient R for the training set and the test set are found to be 0.9897 and 0.9824 for 0°, 0.9897 and 0.9824 for 45° and

0.9897 and 0.9824 for 90°, as shown in Fig. 4. The frequency domain viscoelastic properties in the other orientations can be predicted by rotation transformation.

With the master relationship at a certain temperature, the integral relationships of viscoelasticity can transform each term in the stiffness tensor to a time domain relaxation modulus by numerically integrating Eq. 5 from 0 to infinity.⁴¹

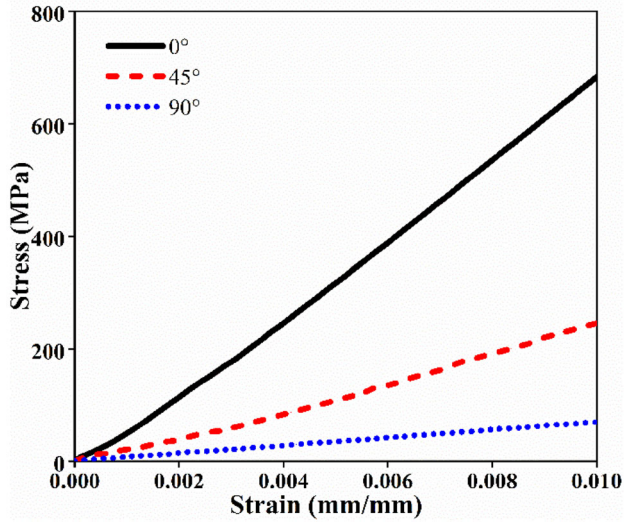


Fig. 3. A representative set of flexural stress–strain curves for unidirectional CFRP laminate tested in 0°, 45° and 90° orientations at 1 mm/s deflection rate. The tests were stopped after acquiring sufficient data for calculating modulus and were not continued to fracture.

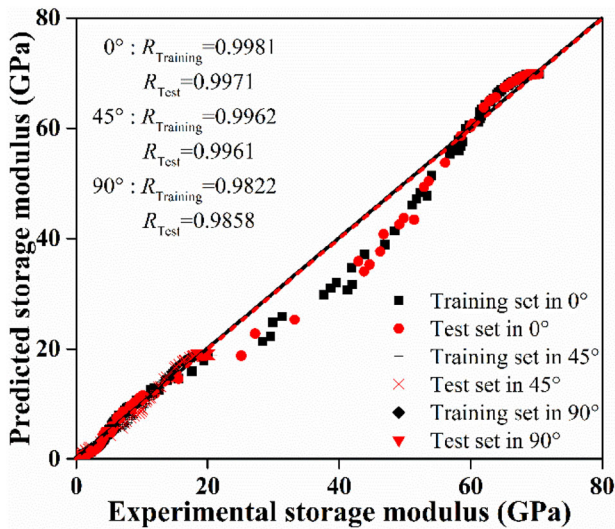


Fig. 4. The Pearson's correlation coefficient R of the experimental and predicted storage modulus values for training and test set in 0°, 45° and 90° orientations.

$$C_{ijkl}(t, T) = \frac{2}{\pi} \int_0^{\infty} \frac{C'_{ijkl}(\omega, T)}{\omega} \sin(\omega t) d\omega \quad (5)$$

where t is time, ω is the angular frequency, and T is the temperature. The relaxation function $C_{1111}(t, T)$ in the 0°, 45° and 90° orientations are shown in Fig. 5. For isothermal processes, $C_{ijkl}(t, T)$ can be used to determine the stress response with a certain strain history by:⁴¹

$$\sigma_{ij}(t, T) = E * \dot{\epsilon} = \int_0^t C_{ijkl}(t - \tau, T) \frac{d\epsilon_{kl}(\tau)}{d\tau} d\tau \quad (6)$$

where τ and $\dot{\epsilon}$ represent time variable and strain rate, respectively. For the standard three-point bending test, the strain rate is assumed to be constant at small deformations, so that Eq. 6 can be approximated as:⁴¹

$$\sigma_{ij}(t, T) = \int_0^t C_{ijkl}(\tau, T) \dot{\epsilon}_{kl} d\tau \quad (7)$$

Using Eq. 7, the stress–strain curve at various temperatures and strain rates can be predicted and the time domain elastic response of the materials can be extracted. The elastic modulus is defined as 0.10% secant modulus. The predicted modulus values with respect to temperature and strain rate are shown in Fig. 6. The elastic modulus decreases with temperature and increases with strain rate. It can also be observed in this figure that the elastic modulus in 0° is also at least 2 times higher than that in 45° and at least 9 times higher than that in 90°, which conforms to the anisotropic nature of the material. To verify the transformation from storage modulus to elastic modulus, the elastic modulus values predicted from the DMA experiment data are extrapolated to room temperature and then compared to those obtained from flexural tests in the 0°, 45° and 90° orientations. The comparisons of the results is shown in Fig. 7. The average errors between the predicted and experimentally measured modulus are found to be below 7.3% in any of the three orientations. The observed variation of the experimental elastic modulus data in 0° orientation testing is attributed to possibilities such as a slight misalignment of the fibers with respect to the loading direction, as a result of cutting the specimens from a large plate, and gripping procedures in the test machine.

The accuracy of model prediction is also tested by predicting the elastic modulus in the 30° orientation using the DMA experiment results in the 0°, 45° and 90° orientations. The predictions are compared to the results from flexural tests in Fig. 8. The average error is found to be 3.4% for this case. The high accuracy proves that the transformation can predict the modulus in any in-plane orientation for a wide range of temperatures and strain rates using a minimum of three specimens. Since the elastic modulus is a widely used material property in mechanical design, the present scheme will significantly reduce the time and effort needed to characterize an anisotropic material. In the present work, the fiber volume fraction and ply stacking

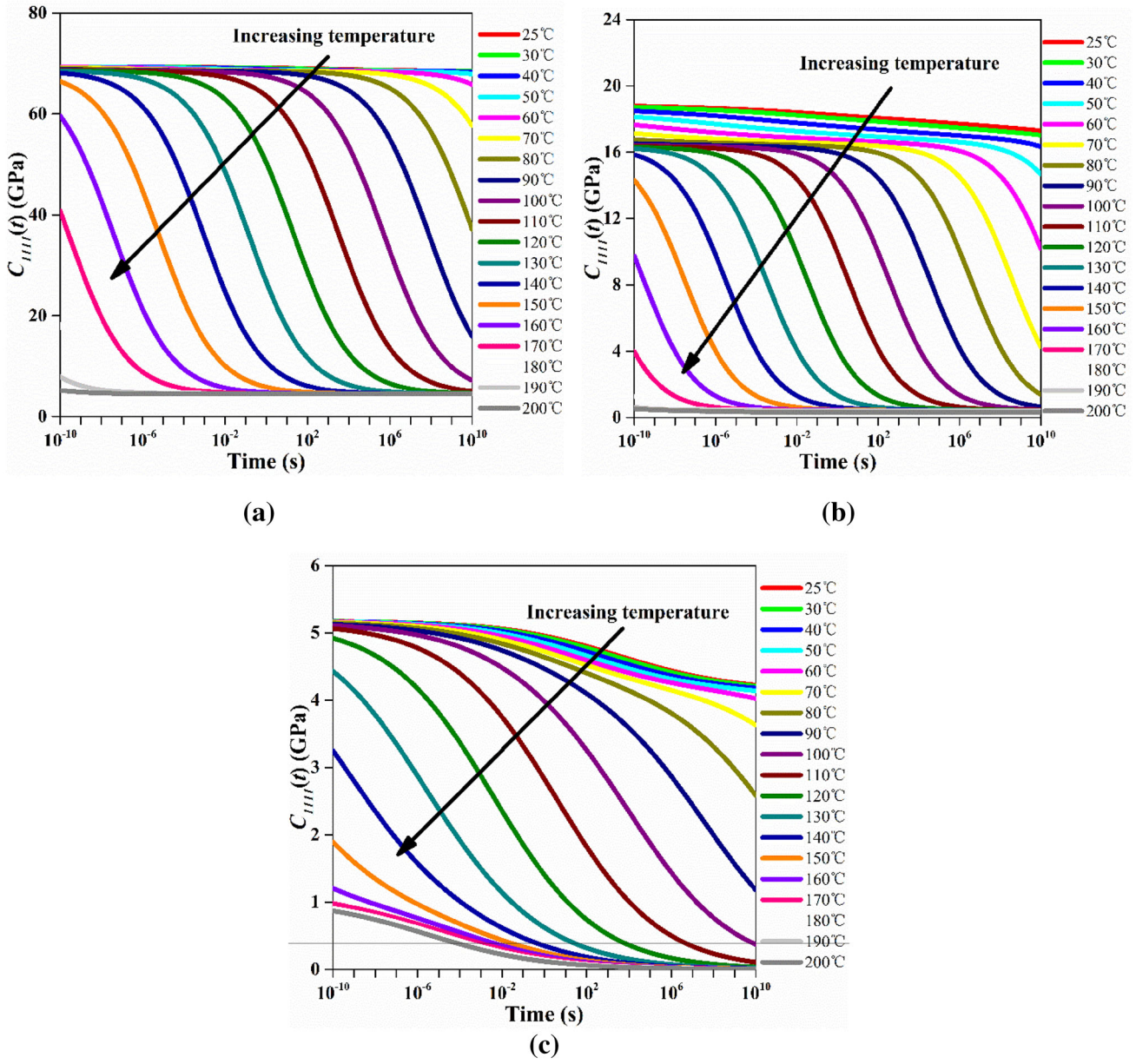


Fig. 5. The relaxation function $C_{1111}(t, T)$ in (a) 0°, (b) 45° and (c) 90° orientations.

sequence are not taken as variables in order to keep the experimental testing campaign manageable for measuring the elastic modulus for validation of the predictions. However, these, and many other parameters, can be taken as variables in the ANN

scheme without any change in the basic framework. The number of neurons in the hidden layer will have to be adjusted based on the number of parameters in a study.

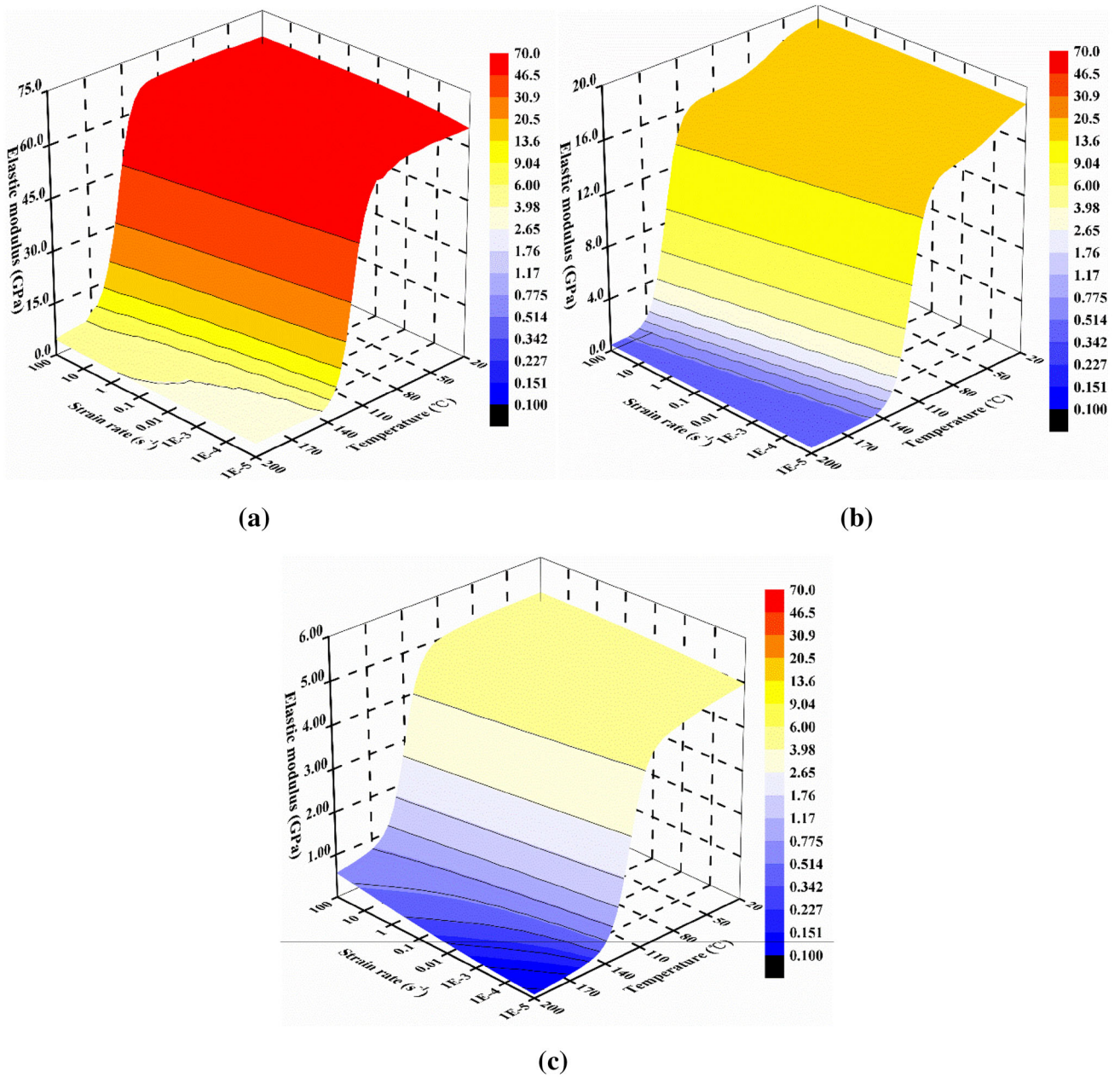


Fig. 6. The predicted elastic modulus of CFRP laminate with respect to temperature and strain rate in (a) 0°, (b) 45° and (c) 90° orientations.

CONCLUSION

An ANN-based transformation has been built to predict the elastic modulus of carbon fiber-reinforced polymer laminate over a wide range of temperatures and strain rates. The DMA results in the 0°, 45° and 90° orientations are used as input to model the directionality. The ANN is trained using a particle swarm optimization algorithm and

converted to a time domain relaxation function using a linear relationship of viscoelasticity. The viscoelastic response is predicted using the relaxation function, and the average error is found to be below 7.3% in the 0°, 45° and 90° orientations. Further validation of the method was conducted to predict the modulus values in the 30° orientation based on the learning of the ANN. The error in prediction of the elastic modulus in the 30°

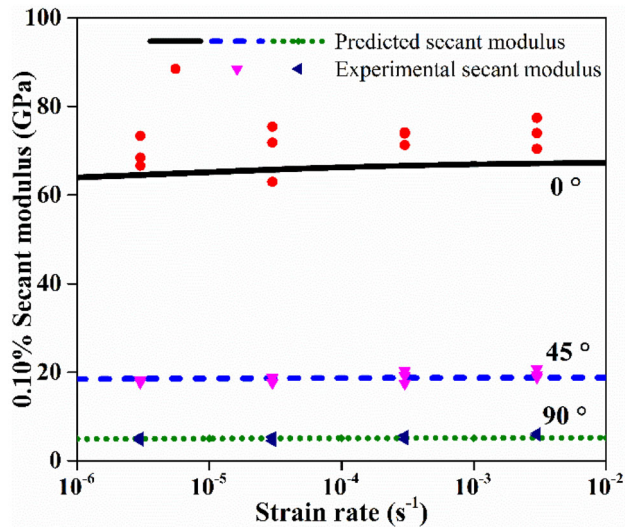


Fig. 7. Comparison of elastic modulus of unidirectional CFRP laminate predicted from ANN approach with experimentally measured values at room temperature (25°C) in 0°, 45° and 90° orientations.

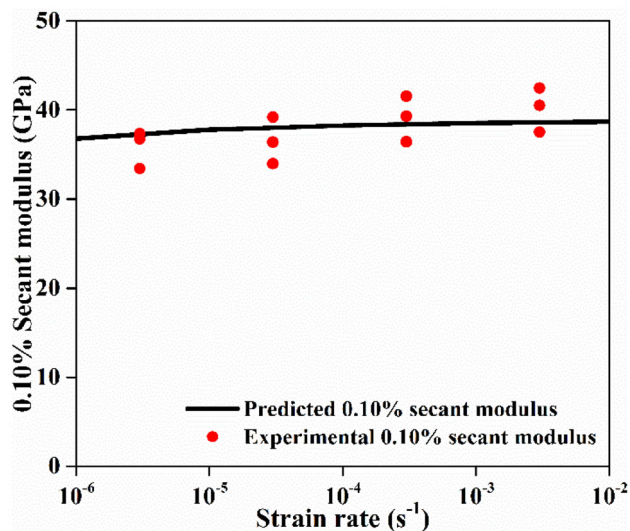


Fig. 8. Comparison of elastic modulus of unidirectional CFRP laminate predicted from ANN and measured from flexural tests at room temperature (25°C) in 30° orientation.

orientation of the laminate was found to be below 3.4%, which shows the effectiveness of the ANN approach for such materials. The high accuracy indicates that the transformation can be used to model and predict the elastic properties of anisotropic materials under a wide range of temperatures and strain rates.

REFERENCES

1. M. Minus and S. Kumar, *JOM* 57, 52 (2005). <https://doi.org/10.1007/s11837-005-0217-8>.
2. R.A. Sullivan, *JOM* 58, 77 (2006). <https://doi.org/10.1007/s11837-006-0233-3>.

3. L. Peroni, M. Scapin, C. Fichera, D. Lehmus, J. Weise, J. Baumeister, and M. Avalle, *Compos. B* 66, 430 (2014). <https://doi.org/10.1016/j.compositesb.2014.06.001>.
4. F. Chen, Y. Luo, N.G. Tsoutsos, M. Maniatakos, K. Shahin, and N. Gupta, *Adv. Eng. Mater.* (2019). <https://doi.org/10.1002/adem.201800495>.
5. A.K. Singh, B. Saltonstall, B. Patil, N. Hoffmann, M. Doddamani, and N. Gupta, *JOM* 70, 310 (2018). <https://doi.org/10.1007/s11837-017-2731-x>.
6. F. Chen, G. Mac, and N. Gupta, *Mater. Des.* 128, 182 (2017). <https://doi.org/10.1016/j.matdes.2017.04.078>.
7. A.K. Singh, B. Patil, N. Hoffmann, B. Saltonstall, M. Doddamani, and N. Gupta, *JOM* 70, 303 (2018). <https://doi.org/10.1007/s11837-017-2734-7>.
8. D. Ivaneiko, V. Toshchevnikov, and M. Saphiannikova, *Polymer* 147, 95 (2018). <https://doi.org/10.1016/j.polymer.2018.04.057>.
9. Z. Jin, K.P. Pramoda, G. Xu, and S.H. Goh, *Chem. Phys. Lett.* 337, 43 (2001). [https://doi.org/10.1016/S0009-2614\(01\)00186-5](https://doi.org/10.1016/S0009-2614(01)00186-5).
10. L.J. Dooling, M.E. Buck, W.-B. Zhang, and D.A. Tirrell, *Adv. Mater.* 28, 4651 (2016). <https://doi.org/10.1002/adma.201506216>.
11. I. Ivaneiko, V. Toshchevnikov, K.W. Stöckelhuber, M. Saphiannikova, and G. Heinrich, *Polymer* 127, 129 (2017). <https://doi.org/10.1016/j.polymer.2017.08.051>.
12. K.P. Sharma, R. Harniman, T. Farrugia, W.H. Briscoe, A.W. Perriman, and S. Mann, *Adv. Mater.* 28, 1597 (2016). <https://doi.org/10.1002/adma.201504740>.
13. P.A. Romero, S.F. Zheng, and A.M. Cuitiño, *J. Mech. Phys. Solids* 56, 1916 (2008). <https://doi.org/10.1016/j.jmps.2007.11.007>.
14. D.D. Luong, D. Pinisetty, and N. Gupta, *Compos. B* 44, 403 (2013). <https://doi.org/10.1016/j.compositesb.2012.04.060>.
15. J.D. Ferry, *Dependence of Viscoelastic Behavior on Temperature and Pressure* (New York: Wiley, 1980), p. 225.
16. S.E. Zeltmann, B.R. Bharath Kumar, M. Doddamani, and N. Gupta, *Polymer* 101, 1 (2016). <https://doi.org/10.1016/j.polymer.2016.08.053>.
17. S.E. Zeltmann, K.A. Prakash, M. Doddamani, and N. Gupta, *Compos. B* 120, 27 (2017). <https://doi.org/10.1016/j.compositesb.2017.03.062>.
18. C. Koomson, S.E. Zeltmann, and N. Gupta, *Adv. Compos. Hybrid. Mater.* 1, 341 (2018). <https://doi.org/10.1007/s42114-018-0026-5>.
19. X. Xu and N. Gupta, *Polymer* 157, 166 (2018). <https://doi.org/10.1016/j.polymer.2018.10.036>.
20. X. Xu and N. Gupta, *Materialia* 4, 221 (2018). <https://doi.org/10.1016/j.mta.2018.09.034>.
21. X. Xu, C. Koomson, M. Doddamani, R.K. Behera, and N. Gupta, *Compos. B* 159, 346 (2019). <https://doi.org/10.1016/j.compositesb.2018.10.015>.
22. X. Xu and N. Gupta, *Adv. Theory Simul.* (2019). <https://doi.org/10.1002/adts.201800131>.
23. E. Vatankhah, D. Semnani, M.P. Prabhakaran, M. Tadayon, S. Razavi, and S. Ramakrishna, *Acta Biomater.* 10, 709 (2014). <https://doi.org/10.1016/j.actbio.2013.09.015>.
24. L.F. Cupertino, O.P.V. Neto, M.A.C. Pacheco, M.B.R. Velasco, and J.R.M. d'Almeida, Modeling the young modulus of nanocomposites: a neural network approach. in *The 2011 International Joint Conference on Neural Networks*, San Jose, California, USA (2011). <https://doi.org/10.1109/ijcnn.2011.6033415>.
25. Z. Sun, E. Ambrosi, A. Bricalli, and D. Ielmini, *Adv. Mater.* 30, 1802554 (2018). <https://doi.org/10.1002/adma.201802554>.
26. P. Jarosz, J. Kusiak, S. Malecki, P. Morkisz, P. Oprocha, W. Pietrucha, and Ł. Sztangret, *JOM* 68, 1535 (2016). <https://doi.org/10.1007/s11837-016-1916-z>.
27. G. Zhao, J. Yang, J. Chen, G. Zhu, Z. Jiang, X. Liu, G. Niu, Z.L. Wang, and B. Zhang, *Adv. Mater. Technol.* 4, 1800167 (2019). <https://doi.org/10.1002/admt.201800167>.
28. O. Sporns, *Adv. Mater.* 5, 488 (1993). <https://doi.org/10.1002/adma.19930050624>.

29. H. Li, Z. Hu, W. Hu, and L. Hua, *JOM* 10, 10 (2019). <https://doi.org/10.1007/s11837-018-03326-2>.
30. D.J. Armaghani, E. Tonnizam Mohamad, E. Momeni, M. Monjezi, and M. Sundaram Narayanasamy, *Arab. J. Geosci.* 9, 48 (2015). <https://doi.org/10.1007/s12517-015-2057-3>.
31. RS Anupama Upadhyay, *OALib J.* 1, 1 (2014). <https://doi.org/10.4236/oalib.1100903>.
32. R.B. Heslehurst, *Compos. Struct.* 35, 369 (1996). [https://doi.org/10.1016/S0263-8223\(96\)00042-6](https://doi.org/10.1016/S0263-8223(96)00042-6).
33. I. Goodfellow, Y. Bengio, and A. Courville, *Deep Learning* (Cambridge, MA: MIT Press, 2016).
34. O.A. Mohamed, S.H. Masood, and J.L. Bhowmik, *Measurement* 107, 128 (2017). <https://doi.org/10.1016/j.measurement.2017.05.019>.
35. J. Kennedy and R. Eberhart, Particle swarm optimization. in *Proceedings of ICNN'95 - International Conference on Neural Networks*, Perth, WA, Australia, 1995. <https://doi.org/10.1109/icnn.1995.488968>.
36. M. Clerc and J. Kennedy, *IEEE Trans. Evolut. Comput.* 6, 58 (2002). <https://doi.org/10.1109/4235.985692>.
37. I.C. Trelea, *Inf. Process. Lett* 85, 317 (2003). [https://doi.org/10.1016/S0020-0190\(02\)00447-7](https://doi.org/10.1016/S0020-0190(02)00447-7).
38. P.J. Angeline, *Evolutionary Optimization Versus Particle Swarm Optimization: Philosophy and Performance Differences* (Berlin: Springer, 1998).
39. Z. Jia, T. Li, F.-P. Chiang, and L. Wang, *Compos. Sci. Technol.* 154, 53 (2018). <https://doi.org/10.1016/j.compscitech.2017.11.015>.
40. R.T.H. Zafer Gürdal and Prabhat Hajela, *Design and Optimization of Laminated Composite Materials* (New York: Wiley, 1999).
41. H. Markovitz, *J. Colloid Interface Sci.* 98, 292 (1984). [https://doi.org/10.1016/0021-9797\(84\)90514-9](https://doi.org/10.1016/0021-9797(84)90514-9).

Publisher's Note Springer Nature remains neutral with regard to jurisdictional claims in published maps and institutional affiliations.